International Journal of
INTELLIGENT SYSTEMS AND APPLICATIONS IN ENGINEERING
ISSN:2147-6799 www.ijisae.org Original Research Paper

Multi-DGPV Planning Using Artificial Intelligence

[1]Azlina Abdullah, [2]**Ismail Musirin, [3]Muhammad Murtadha Othman, [3]Siti Rafidah Abdul Rahim, [4]A.V. Sentilkumar

Submitted: 13/11/2022 **Accepted**: 14/02/2023

Abstract: This article investigates the impact of multi-Distributed Generation Photovoltaic (DGPV) installation and their degree of penetration on controlling power loss in the radial distribution system. The Integrated Immune Moth Flame Evolution Programming (IIMFEP), a unique hybrid optimization technique, was utilized to identify the ideal DGPV size and location for base case conditions and under load variations. The IIMFEP approach is compared against Evolutionary Programming (EP), Artificial Immune System (AIS), and Moth Flame Optimization (MFO) and validated using the IEEE 118-Bus Radial Distribution Systems (RDS). Incorporating multi-DGPV into a system reduces the total real and reactive power loss while simultaneously increasing the minimum voltage and decreasing the total voltage deviation. In every instance examined in this study, the IIMFEP method yields optimal solutions superior to those generated by the other three methods. As the number of DGPV units increased to nine, the percentage of power loss reduction became the highest among all DG units examined, and DG penetration reached 94.26 percent. This research provides the power system operator with comprehensive findings demonstrating the impact of installing multi-DGPV in distribution networks on system loss.

Keywords*: Optimization; Loss minimization; Distributed generation; Evolutionary programming; Distributed generation photovoltaic; Backward forward sweep; Total voltage deviation*

1. Introduction

In view of the recent deregulation and increasing environmental awareness, the integration of distributed generation (DG) into the distribution system is becoming a viable option for distribution network operators (DNO) to enhance system performance.

Integration of DG into the distribution network that is meticulously planned provides a number of benefits. The following are the benefits: active and reactive power loss reduction [1], [2], voltage stability improvement [3], [4], reliability improvement, pollution emissions reduction [5], increasing system reliability, enhanced system security, and maximization of profit [6], [7]. However, due to the intermittent nature of renewable energy (RE), the DNO find it challenging to integrate RE into their systems. The complexity of the unidirectional power flow between the substation and the consumers causes an imbalance in the system's addition of RE power. The penetration of an RE system into the grid introduces voltage regulation, frequency regulation, reverse power flow, harmonics, and other issues [8]–[11]. As a result, rigorous planning of the power system with the presence of RE is required. However, the mere location and size of these devices might not benefit the system. It is critical to place the DG in a way to maximize system benefits.

Numerous studies have adopted techniques and algorithms to address diverse problems, including the DG allocation problem. Babu et al. [12] presented the Harris Hawk optimization method to determine the ideal placements and sizes of various types of DGs in a radial distribution system (RDS). Zulkiffli et al. [13] utilize the Loss Sensitivity (LS) method to determine the appropriate DG locations and the Firefly Algorithm (FA) to calculate the optimal DG capacity in an attempt to improve the system's voltage stability. Another important work that can be highlighted is the work in [14]which addresses the application of the Improved Marine Predators algorithm (IMPA) to incorporate both real and reactive power resources into distribution systems with the goal of minimizing total reactive power losses. The authors of proposed [15] the Immunized Brainstorm Evolutionary Programming (IBSEP) to illustrate the impact of installing various DG types.

Meanwhile, the study in[16] determined that the Fruit fly method provides a better power factor than the cat swarm strategy for calculating the power factor of wind-based DGs in order to reduce harmonics in the distribution system. The artificial Bee Colony (ABC) method has been used in [17] for the DG location and sizing problem, with three

1Department of Engineering Foundation and Diploma Studies, College of Engineering, Universiti Tenaga Nasional,43000 Kajang, Selangor, Malaysia.
e-mail: aazlina@uniten.edu.my
2Institute for Biodiversity and Sustainable Development (IBSD),Universiti Teknologi MARA (UiTM) 40450 Shah Alam, Selangor, Malaysia. School for Surveying Science and Geomatics College of Built Environment, Universiti Teknologi MARA 40450 Shah Alam, Selangor, Malaysia.
3e-mail: ismailbm@uitm.edu.my, m_murtadha@uitm.edu.my
Faculty of Electrical Engineering Technology, Universiti Malaysia Perlis, Kampus Pauh Putra, 02600, Arau, Perlis, Malaysia
e-mail: rafidah@unimap.edu.my
4Hindusthan College of Arts and Science,Coimbatore, India.
Email: avsenthilkumar2007@gmail.com
***Corresponding author: ismailbm@uitm.edu.my*

objectives: total power losses, total energy cost, and average voltage drop. Another study in [18] applied the multi-objective Chaotic Mutation Immune Evolutionary Technique (MOCMIEP) to investigate the ideal sizing and positioning of DGPV to reduce total power losses concurrently and improve the voltage stability index. Duong et al. [19] integrate chaos into the original Stochastic Fractal Search (SFS) technique, employing ten prominent chaotic maps to solve the optimal DG allocation issue in RDS. The results indicate that the proposed Chaotic mutation chaotic local search (CMSFS) provides a solution superior to the SFS.

The Integrated Immune Moth Flame Evolutionary Programming (IIMFEP) method, which incorporates Artificial Immune System (AIS) and Moth Flame Optimization (MFO) inside the framework of Evolutionary Programming (EP), was utilized to optimize the locations and sizes of multiple DG-PVs in base case conditions and under load variations to minimize total system loss. The proposed technique has been evaluated on the IEEE-118 Bus RDS, and the results are compared to those of EP, AIS, and MFO algorithms. The reported results indicate that the proposed technique outperforms EP, AIS, and MFO algorithms in terms of reducing overall system loss.

The following are the key accomplishments of this work:

• Proposing a novel hybrid optimization method IIMFEP, based on chaotic local search rather than gaussian mutation.

• Using the proposed IIMFEP to determine the ideal siting and sizing of multi DGPV units in an RDS in base case condition to minimize total active power losses while improving the voltage profile.

• Using the proposed IIMFEP to determine the ideal siting and sizing of multi DGPV units in an RDS under load variations to minimize total active power losses while improving the voltage profile

• Comparing the efficacy of the proposed methodology to the EP, AIS, and MFO methods using 118-Bus distribution systems.

The remaining sections of this work are organized as follows. Section II introduces the mathematical formulas for optimal DG allocation problems. Section III describes the algorithms that have been proposed. Case studies and simulation outcomes are presented in Section IV. Section V concludes with the conclusion.

2. Problem Formulation

A. Load Flow Analysis

Power systems are analyzed by efficient algorithms and software. Regardless of the goal function, load flow analysis is required prior to placing DG in the distribution system. The task should be completed without violating the system constraints. The traditional Newton-Raphson, Gauss-Seidel, and Fast Decoupled Load Flow methods are widely used in transmission system analysis because of their efficiency, but they are far less effective in distribution system analysis [20].

A backward Forward Sweep (BFS) based algorithm has become the most widely used method for calculating distribution power flow [21], [22]. The primary characteristics of this power flow method are its simplicity, speed, low memory requirements, and robust convergence in the RDS solution. BFS relies on a backward and forward cycle at each iteration as its core operating principle. The initial phase of BFS is to calculate the load current at each node for each iteration, which can be done as follows:

$$I_{load\_t}^{(\ell)} = conj\left(\frac{S_t}{V_t^{(\ell-1)}}\right) \; for\; t = 2 \ldots N \tag{1}$$

Where ℓ represents the iteration number, t is the node/bus, $I_{load\_t}^{(\ell)}$ is the load current at node t on iteration ℓ, S_t is the power injection at node t, $V_t^{(\ell-1)}$ is the voltage of node t calculated from the previous iteration and N is the total number of nodes. The second phase is the backward sweep, which calculates the branch currents of all branches. The branch current is computed beginning at the end node and moving toward the source node using an expression (2).

$$I_{t-1,t}^{(\ell)} = I_{load\_t}^{(\ell)} + \sum I_{t,t+1}^{(\ell)} \tag{2}$$

Where, $I_{t-1,t}^{(\ell)}$ represents the branch current connecting node t to its upstream node $t-1$ and $\sum I_{t,t+1}^{(\ell)}$ is the total of branch currents emanating from node t. The third phase is the forward sweep, which involves calculating the bus voltages for each node. The bus voltage is computed from the source node to the end node using (3).

$$V_t^{(\ell)} = V_{t-1}^{(\ell)} - Z_{t-1,t}\, I_{t-1,t}^{(\ell)} \tag{3}$$

Where $V_t^{(\ell)}$ is the voltage of node t at iteration ℓ, $V_{t-1}^{(\ell)}$is the voltage of the immediate upstream node of node t, and $Z_{t-1,t}$ is the branch impedance connecting node t to its immediate upstream node.

The next phase is to calculate the magnitudes of the voltage error. It is achieved by tracking the voltage magnitude differences at each node between two successive iterations. The maximum voltage error is then determined by taking the maximum value of all voltage error magnitudes at all nodes (other than node 1) for the current iteration of ℓ. The BFS stops when the conditions specified in (4) are met.

$$e_{max}^{(\ell)} \leq E_{tol}(tolerance) \tag{4}$$

where $e_{max}^{(\ell)}$ is the maximum error at iteration ℓ, and $E_{tol}(tolerance)$ is the tolerance limits.

B. Objective Function

The objective function *OF* of this study is to minimize the loss in the distribution system, which is mathematically represented by (5).

$$OF = \min(P_{LOSS}) \quad (5)$$

The active and reactive power loss in the line section between buses *m* and *n* are calculated as in (6) and (7).

$$P_{loss\_mn} = I_{mn}^2 \times R_m \quad (6)$$

$$Q_{loss\_mn} = I_{mn}^2 \times X_m \quad (7)$$

The total active power losses (APL) and reactive power losses (RPL) of the distribution systems can be determined by adding all line section losses, given by (8) and (9).

$$P_{LOSS} = \sum_{j=1}^{N_{line}} P_{loss\_mn} \quad (8)$$

$$Q_{LOSS} = \sum_{j=1}^{N_{line}} Q_{loss\_mn} \quad (9)$$

Where:

I_{mn} = current magnitude at branch *m* and *n*

j = branch number

R_m = resistance at branch *m*

X_m = reactance at branch *m*

N_{line} = maximum number of branches

Power loss can also be stated as a percentage (%) when comparing results, termed as power loss reduction percentage (PLRP) as shown in (10):

$$PLRP = \frac{Ploss_{without\_DG} - Ploss_{with\_DG}}{Ploss_{without\_DG}} \text{ x } 100 \quad (10)$$

The objective function is mainly subjected to voltage and DG size constraints during the optimization process. During injecting DG into the system, the voltage magnitude at each bus must remain within the prescribed limit[23].

$$0.95 \text{ p.u.} \leq V_t \leq 1.05 \text{ p.u.} \quad (11)$$

To reach a fair solution, the size of the DG cannot be too small or too large relative to the system's load value. The amount of active and reactive power generated by each DG unit must range between 10 and 80 percent of the system's total load demand [24].

10% of total active load demand ≤ P_{DG_t} ≤ 80% of total active load demand (12)

10% of total reactive load demand≤ Q_{DG_t} ≤ 80% of total reactive load demand (13)

Where V_t is the voltage magnitude at bus *t*, and P_{DG_t} and Q_{DG_t} are the DG active and reactive power components injected at the *t-th* bus. Total Voltage Deviation (TVD) is calculated as follows [25]:

$$TVD = \sum_{t=1}^{N} |V_t - V_{ref}| \quad (14)$$

Penetration level is calculated as follow [15]:

$$\text{Penetration Level} = \frac{\text{Total installed DGPV capacity}}{\text{Total active load demand}} \text{ x } 100 \quad (15)$$

The effect of installing three DGs Type I under load variations are investigated. The following equation determines the load variation from no-load to full-load[14].

$$P_{jnew} + jQ_{jnew} = K\,(P_j + jQ_j) \quad (16)$$

Where K= [0.6, 0.8, 1.0, 1.2, 1.4 and 1.6] is the load factor. For each load step modification, the power system feeder loads are varied from 60%, 80%, 100%, 120%, 140% and 160% from the base case, while the optimal size and location of DG are computed using EP, AIS, MFO, and IIMFEP.

3. Overview of the Proposed Method

This section proposes the IIMFEP optimization technique for addressing the placement of multiple DGPVs on IEEE-118 Bus RDS to minimize active power loss. AIS and MFO features are incorporated into the EP approach to creating the IIMFEP. Based on a review of the relevant literature, it has been determined that combining them with other algorithms could make them more effective and resilient. The complete flow chart for the IIMFEP algorithm is represented in Figure1.

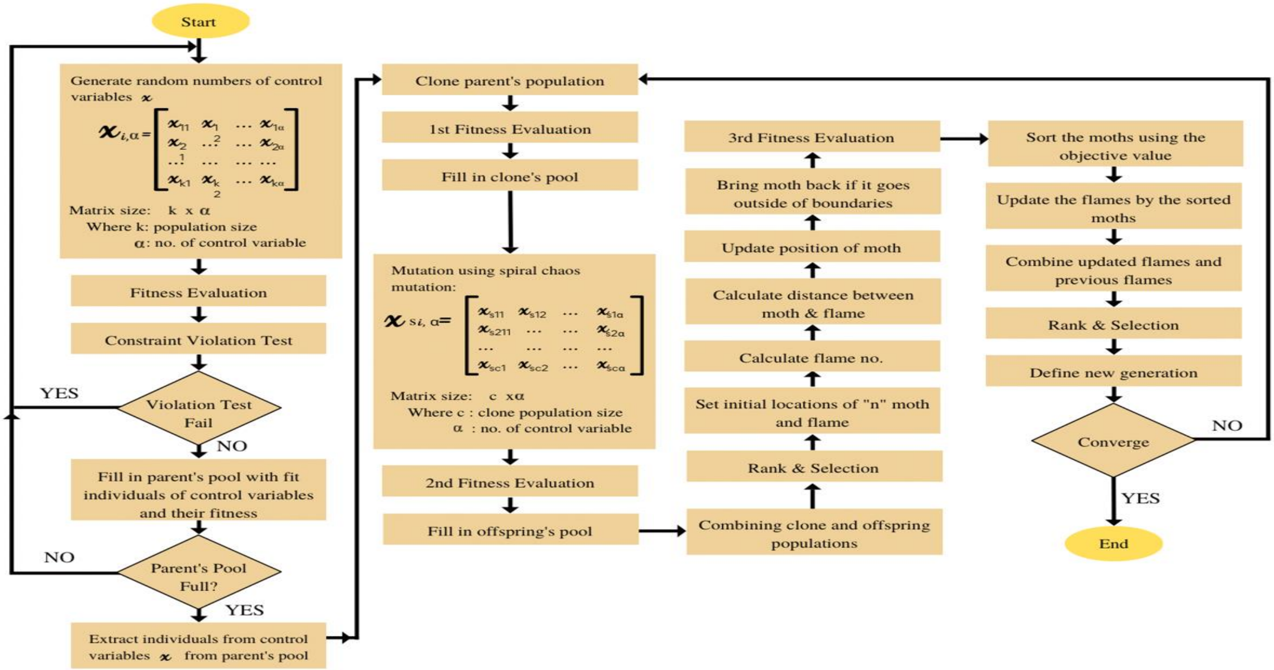

Fig. 1 Flowchart for proposed IIMFEP.

The initialization process is the first step in the IIMFEP algorithm. In this procedure, the number of individuals, the size of each mutation step, the number of clones, and the maximum number of iterations had to be set. In this process, a population of candidates is generated using random numbers. During the pre-fitness computation process, the fitness value of the random population is then calculated. Individuals who violate the requirement are exterminated from the population. The accepted population is referred to as the parents' population. The population of the parents is cloned by a chosen factor that multiplies these candidates. Cloned populations are used to produce offspring, bred during a mutation. In the mutation process, Chaotic Local Search (CLS) mutation with a circle map function is used to produce offspring [26]. The offspring are produced by mutating the cloned population on the CLS operator specified in (17). X_{mut} is a new candidate solution or offspring.

$$X_{mut} = (1 - \lambda) * X_{clone} + \lambda * CH_i \quad (17)$$

Where $i = 1, . . . , K$, λ is a shrinking factor, which is defined as follows:

$$\lambda = (max_{cycle} - \ell + 1) / max_{cycle} \quad (18)$$

Here max_{cycle} is the maximum number of iterations, and ℓ is the number of iterations. CH_k is the chaotic vector in the interval $[l, u]$, derived from:

$$CH_k = LB + chaos_k * (UB - LB) \quad (19)$$

Where $i = 1, . . . , K$, UB and LB are the lower bound and upper bound of variable X, respectively. The individual produced by the circle map function, $chaos_k$ is calculated as follows:

$$chaos_{k+1} = \{ chaos_k + \mathrm{b} - (\mathrm{a}\ 2\pi) \sin (2\pi\ chaos_k)\} \bmod (1) \quad (20)$$

Where $chaos_{k+1}$ is a new vector of the individual in *a k-th* generation produced by the circle map function, a = 0.5 b = 0.2, k is the length of a chaotic sequence, and $ch0 \in (0, 1)$ is a random number. The fitness value of the offspring is then computed during the fitness two calculation. The cloned and offspring populations are merged into a single population via a combination process. A tournament system is used to determine the healthiest individuals in a population. First, the combined population is ranked, the top two-thirds healthiest individuals are chosen, and the remainder is removed. The moth population is then comprised of the top two-thirds of individuals. Once the moth and flame is initialized, the number of flames is computed as follows:

$$\text{flame } number = round\ (N_{flame} - \ell * \frac{N_{flame} - 1}{T}) \quad (21)$$

The moth population is then updated using spiral equation:

$$\mathrm{S}(M_i, F_j) = D_i \,.\, e^{bd} . \cos(2\pi \mathrm{t}) + F_j \quad (22)$$

Then the algorithm constant *b* and *d* is updated. Constant *b* is the constant that defines the shape of a logarithmic spiral, and *d* is the random number in [*r*,1], where *r* is decreased linearly from -1 to -2. The distance between the moth and the flame is then computed as follows:

$$D_i = | F_j - M_i| \quad (23)$$

Where N_{flame} represents the maximum number of flames, T represents the maximum number of iterations, ℓ is the current number of iterations, F_j indicates the *j-th* flame, and M_i indicate the *i-th* moth. Fitness 3 calculates the fitness of the updated moths. The moths are then sorted based on their fitness using a ranking mechanism. The sorted moths are known as flames. The next stage combines new and old flames to create a new population. After ranking the entire population, just the 20 healthiest individuals are picked using a tournament process, and the rest are eliminated. Individuals chosen in the selection process are the Parents for the next iteration. The convergence test evaluates if the IIMFEP algorithm can be stopped when it reaches the maximum iterations. If convergence conditions are not met, the whole process will repeat.

4. Results and Discussion

The proposed IIMFEP is tested using the IEEE 118-Bus RDS to determine the optimal DG sizing and location in this study. In each scenario, the performance of the system, such as total real power loss (P_{LOSS}), total reactive power loss (Q_{LOSS}), minimum voltage (V_{min}), penetration level, and total voltage deviation, are calculated. The performance of the IIMFEP is compared to that of the EP, AIS, and MFO algorithms in terms of minimizing distribution losses while meeting the system's voltage constraint. The size and location of DGs in the power system are thoroughly investigated utilizing one, three DGs, five DGs, seven DGs, and nine DGs. Then, the impact of multi-DG type I installations on the 118-Bus RDS during load changes are further investigated using the proposed method. In this case, DG Type 1, i.e., the PV is considered for the installation. The results of multi-DGPV installation have been compared with the results from pre-DGPV installation.

The 118-Bus RDS consists of 118 buses and 117 branches, as shown in Figure 2. The line data and load data are taken from [27], where the bus number are rearranged. The rated voltage is 11 kV and the substation voltage is considered one p.u.. The total real and reactive demand on the system is 22,709.70 kW and 17,041.10 kVAr respectively. In this study, it is more relevant to assume all loads are constant power loads. The population size for each of the four optimization methods is twenty. Meanwhile, the maximum number of iterations, max_{cycle} for DGPV units installation need to be tuned manually [19]. For the installation of three to five DGPV units, the max_{cycle} selected is 200, but for the installation of seven to nine DGPV units, the max_{cycle} is 400.

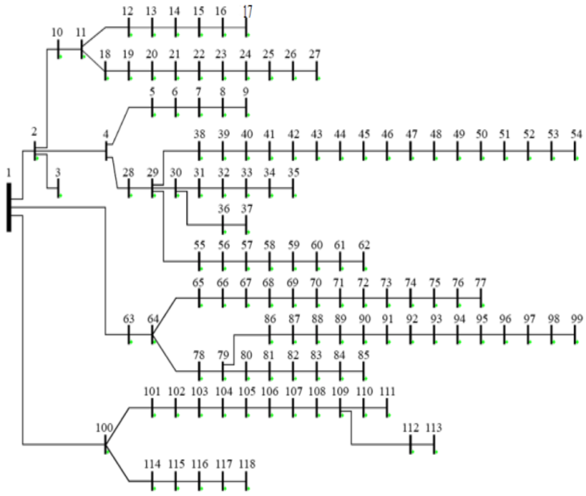

Fig. 2 The IEEE 118-Bus RDS.

C. Pre-DG Installation

In order to study the effectiveness of the proposed method, the total losses at the base case were calculated without DGPV installation. Table 1 presents the results of a Backward/Forward Sweep load flow operation for an uncompensated 118 test system without DG installation.

Table 1. Pre-DGPV Installation.

P_{LOSS} (kW)	Q_{LOSS} (kVAr)	V_{min}	TVD
1298.07	978.72	0.8688 p.u. at bus 77	5.373 p.u.

From Table 1, the minimum voltage of 0.8688 p.u. is observed at bus 77 for 118-Bus RDS [28], which is below the prescribed limit of the voltage magnitude constraint. Moreover, the total real power loss of the system is 1298.07 kW, the total reactive loss of the system is 978.72 kVAr, and TVD is 5.373 p.u.

D. Single DGPV Installation

Manual search, EP, AIS, MFO, and IIMFEP approaches are used to determine the optimal size and placement for a single DGPV installation. The top 10% of the weakest bus for the base case without DG installation is identified and listed in Table 2 for the manual search technique. These bus numbers were chosen as the primary site of the system's single DG. The real power of the DG is then varied from 0 kW to 10 kW at 10 kW intervals for each potential site of the DG. Figure 3 shows the overall power loss of the system as the DG size is adjusted from 0 kW to 10 kW for all possible sites. The graph shows that the lowest total APL is obtained when the DG size is ideal. However, losses grow as DG size increases above the optimal size, eventually exceeding overall losses without DG installation. Failure to identify the optimal size and location of DG will cause an increase in power loss. Figure 4 depicts a magnification of Figure 3 for

2500 kW to 3000 kW DG size. The optimal size of DG that caused the least amount of power loss at all potential locations is then recorded in Table 3. It is discovered that the optimal size of DG is 2980 kW, which must be installed at bus 71 in order to attain the system's lowest overall APL of 1016.69 kW.

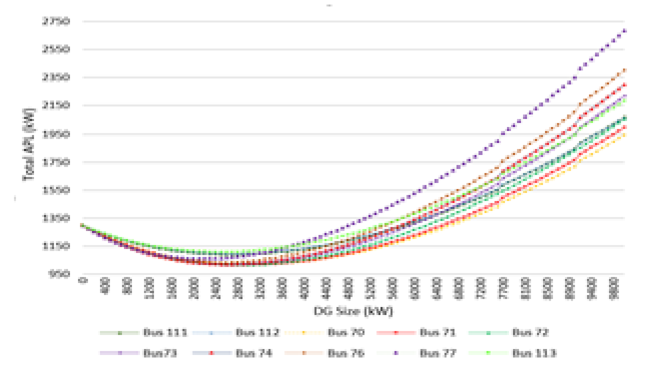

Fig. 3 Total Active Power Losses for DG Size vary from 0 kW to 10kW at Potential DG Locations

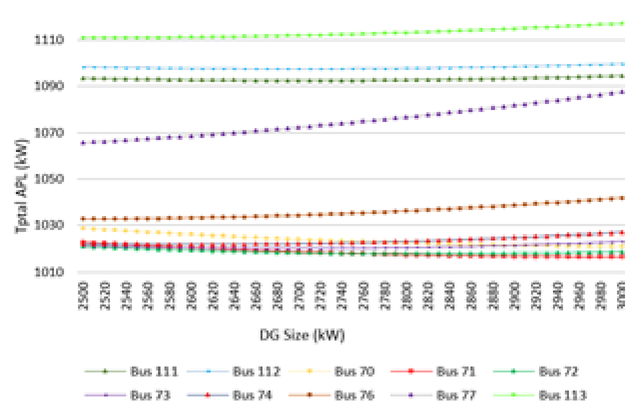

Fig. 4 Zoom in of the region 2500kW to 3000 kW.

Table 2. Bus Voltages for the Top 10% of the Weakest Buses.

Bus	Voltage (p.u.)
77	0.8688
76	0.8689
75	0.8706
74	0.8714
73	0.8748
72	0.8792
71	0.8840
70	0.8877
111	0.9053
113	0.9071
112	0.9072

Table 3. The Optimal Size of DG Resulted in the Minimum Power Loss at All Potential Sites

Loc.	Size of DG (kW)	Vmin (p.u.)	P_{LOSS} (kW)	Q_{LOSS} (kVAR)
111	2700	0.8688	1092.52	865.41
112	2700	0.8688	1097.52	867.28
70	3050	0.9053	1021.02	777.05
71	2980	0.9053	1016.69	775.99
72	2980	0.9053	1016.69	776.70
73	2690	0.9053	1020.28	780.54
74	2600	0.9053	1021.94	782.85
76	2480	0.9053	1032.70	788.59
77	2180	0.9053	1061.45	803.51
113	2510	0.8688	1110.98	873.76

The manual search method is limited to exhaustive examination. As the number of DG expanded, the manual search technique to determine DG's optimal size and location became impractical. In order to find the ideal size and location of DG to minimize power loss, an optimization method is necessary. Table 4 shows the simulation results obtained using EP, AIS, MFO and IIMFEP optimization techniques for single DGPV installation in 118-Bus RDS.

For single DGPV installation, IIMFEP performance is comparable to MFO performance by producing the same total real power loss, which is 1016.9 kW with a 21.68% of power loss reduction. The total APL obtained from IIMFEP and MFO is similar to the total APL obtained using a manual search. Meanwhile, EP and AIS produce 1090.15 kW and 1090.26 kW of total power losses with 16.02% and 16.01% of power loss reduction percentages. The DG size with a single DG installation is 3816.5 kW, 3817.5 kW, 2978.55 kW, and 2978.52 kW for EP, AIS, MFO, and IIMFEP, respectively. EP and AIS have identified location bus 75 for DG placement, while MFO and IIMFEP have identified location bus 71.

E. Multi DGPV Installations

The size and siting of DG-PVs in the power system are thoroughly examined, with 3,5,7 and 9 DGs. Table 5,6,7 and 8 compares and contrasts the findings of EP, AIS, MFO, and IIMFEP when 3, 5, 7 and 9 DGPVs are installed in the system, respectively. For multi-DGPV installations, the IIMFEP strategy beat the other three techniques. In a three-unit DG-PV installation, the IIMFEP has the lowest total real power loss at 667.28 kW, followed by the MFO, EP, and AIS with 675.03 kW, 943.9 kW, and 944.36 kW, respectively.

Using the proposed IIMFEP as an optimization technique, the total reactive power loss was decreased from 978.72 kVAr to 507.05 kVAr, the total voltage deviation was decreased from 5.37 p.u. to 3.11 p.u., and the minimum voltage was improved from 0.8688 p.u. prior to DG installation to 0.9540 p.u. after 3 DGPV installations, which was above the minimum voltage constraint.

Table 4. Simulation Results of EP, AIS, MFO and IIMFEP for Single DGPV Installation in 118-Bus RDS

		EP	**AIS**	**MFO**	**IIMFEP**
SINGLE DGPV	P_{LOSS} (kW)	1090.15	1090.26	1016.69	**1016.69**
	Q_{LOSS} (kVAr)	803.28	803.33	776.00	775.98
	V_{min} p.u.	0.9053	0.9053	0.9053	0.9053
	TVD p.u.	3.907	3.907	4.237	4.236
	PRLP	16.02%	16.01%	21.68%	21.68%
	P_{DG} (kW) / Bus	3816.50 (75)	3817.92 (75)	2978.55 (71)	2978.52 (71)
	Total P_{DG} (kW)	3816.50	3817.92	2978.55	2978.52

Table 5. Results of EP, AIS, MFO and IIMFEP for Three-DGPV Installations in 118-Bus System

		EP	**AIS**	**MFO**	**IIMFEP**
THREE DGPVs	P_{LOSS} (kW)	943.9	944.36	675.03	**667.28**
	Q_{LOSS} (kVAr)	712.71	713.47	512.82	507.05
	V_{min} p.u.	0.9115	0.9113	0.9514	0.9540
	TVD p.u.	3.833	3.842	3.170	3.110
	PRLP	27.29%	27.25%	48.00%	48.60%
	P_{DG} (kW) /Bus	2626.77 (106) 3125.76 (56) 4509.43 (67)	2592.03 (106) 3106.22 (56) 4486.15 (67)	2702.30 (111) 3015.72 (49) 2985.47 (71)	2978.57 (71) 3119.86 (109) 2883.17 (50)
	Total P_{DG} (kW)	10261.97	10184.39	8703.49	8981.6

Table 6. Results of EP, AIS, MFO and IIMFEP for Five-DGPV Installations in 118-Bus System

		EP	**AIS**	**MFO**	**IIMFEP**
Five DGPVs	P_{LOSS} (kW)	845.98	846.05	584.37	**581.57**
	Q_{LOSS} (kVAr)	723.26	723.31	444.81	435.11
	Vmin p.u.	0.9163	0.9163	0.9543	0.9548
	TVD p.u.	3.332	3.332	2.551	2.672
	PLRP	34.83%	34.82%	54.98%	55.20%
	P_{DG} (kW) /Bus	2718 (42) 2519.98 (112) 5647.18 (9) 6069.43 (63)	2719.29 (42) 2521.61 (112) 5649.21 (9) 6071.78 (63)	2271.00 (40) 2271.00 (96) 2745.01 (50) 2869.32 (110)	2857.79 (71) 6454.16 (29) 2512.90 (50) 2520.11 (79)

		3386.97 (69)	3388.16 (69)	2555.00 (72)	3118.73 (109)
	Total P_{DG} (kW)	20341.57	20350.05	12711.33	

Table 7. Results of EP, AIS, MFO and IIMFEP for Seven-DGPV Installations in 118-Bus System

		EP	**AIS**	**MFO**	**IIMFEP**
Seven DGPVs	P_{LOSS} (kW)	723.6	723.71	540.05	**527.07**
	Q_{LOSS} (kVAr)	528.52	528.61	417.07	397.25
	Vmin p.u.	0.9370	0.9370	0.9493	0.9543
	TVD p.u.	2.210	2.209	2.298	2.077
	PLRP	44.26%	44.25%	58.40%	59.40%
	P_{DG} (kW) /Bus	3431.65 (78) 2749.42 (112) 2700.78 (18) 2408.22 (33) 2578.25 (38) 3220.04 (48) 4524.47 (68)	3432.11 (78) 2750.47 (112) 2701.35 (18) 2408.74 (33) 2578.95 (38) 3221.13 (48) 4525.95 (68)	2271.00 (40) 4769.81 (4) 2362.39 (74) 4280.43 (91) 2271.00 (50) 2377.37 (80) 2271 (110)	2270.97 (40) 2699.48 (50) 2270.97 (96) 2869.17 (110) 2270.97 (80) 2270.97 (20) 2612.53 (71)
	Total P_{DG} (kW)	21612.84	21618.7	20602.99	17265.07

Table 8. Results of EP, AIS, MFO and IIMFEP for Nine-DGPV Installations in 118-Bus System

		EP	**AIS**	**MFO**	**IIMFEP**
Nine DGPVs	P_{LOSS} (kW)	732.29	857.92	527.95	**511.43**
	Q_{LOSS} (kVAr)	587.81	657.84	404.82	382.15
	Vmin p.u.	0.9175	0.9515	0.9495	0.9547
	TVD p.u.	2.416	1.775	2.1707	1.999
	PLRP	43.59%	33.91%	59.33%	60.60%
	P_{DG} (kW) /Bus	3422.32 (78) 3674.42 (41) 6702.74 (63) 3189.35 (3) 3263.46 (111) 2589.20 (11) 2422.65 (103) 3352.48 (4) 2741.66 (71)	4288.42 (82) 2674.52 (42) 3385.65 (109) 3310.87 (21) 5198.78 (7) 2484.31 (76) 2320.31 (86) 2776.88 (66) 2702.99 (48)	2270.97 (2) 2270.97 (2) 2270.97 (40) 3119.94 (109) 2270.97 (96) 2270.97 (80) 2270.97 (11) 2270.97 (74) 2270.97 (50)	2496.91 (30) 2270.97 (20) 2334.28 (50) 2270.97 (2) 2270.97 (91) 2351.28 (73) 2270.97 (40) 2868.88 (110) 2270.98 (79)
	Total P_{DG} (kW)	31358.25	29142.73	21287.70	21406.22

The locations and sizing of all the DG-PVs are also given in the tables. For instance, when 9 DG-PV units are installed in the system; the sizing of the individual DG is 2496.91 kW, 2270.97 kW, 2334.28 kW, 2270.97 kW, 2270.97 kW, 2351.28 kW, 2270.97 kW, 2868.88 kW and 2270.98 kW; which need to be installed at buses 30, 20, 50, 2, 91, 73, 40, 110 and 79. All the optimal locations are shown in the bracket as highlighted in the box of Table 8 for 9 DG-PV installations.

As the number of DGPVs is incrementally increased up to nine DGPVs, the total real and reactive power are reduced, the minimum voltage is enhanced, and the TVD continues to decrease. As shown in Table 8 and Figure 5, the case for 9 DGPV installations in the system has the lowest total real power loss, as the total loss has been reduced to 511.43 kW using the IIMFEP as highlighted in the table. Figure 5 depicts the total real power loss and PLRP derived by the IIMFEP method for 1, 3, 5, 7 and 9 DGPV installations. The PLRP continues to climb when the number of DGs installed in the system increases. The maximum PLRP occurs when 9 DGPVs are installed in the system. However, the percentage difference between seven and nine DGs is only 1.2 percent.

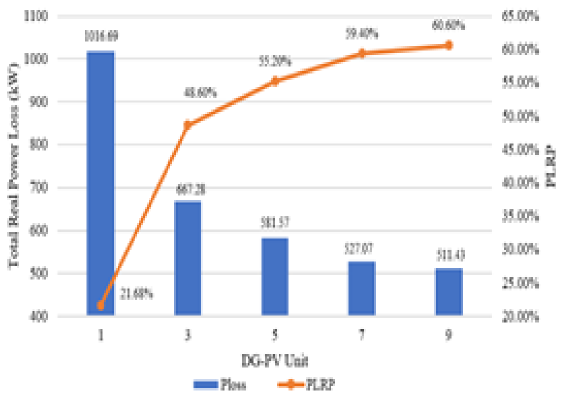

Fig. 5 Total real power loss And PLRP Obtained for Multi-DGPV Installation using IIMFEP Technique in

To keep the system's real power loss as low as possible, the total DGPV capacity must be raised, and additional DG units must be installed, as seen in Figure 6. For the largest reduction of power loss, a DGPV penetration of 94.26% is required

Figure 7 illustrates the voltage boost in the system caused by the IIMFEP approach for multi-DGPV installation in the system. The lower the TVD number, the closer the bus voltage is to its nominal value in this instance (i.e., 1.0 p.u.). According to the table, the TVD for seven DGs is 2.157 p.u.. In addition, the TVD for nine DGs is 2.000 p.u.. In Figure 8, the voltage profiles of the system, when installed with seven and nine DGs, are denoted by red and black lines at the extremes of the radar graph. It shows that the bus voltages are approaching the nominal value. The voltage profile of the system with DG installations is enhanced when compared to the voltage profile of the system without DG adjustment.

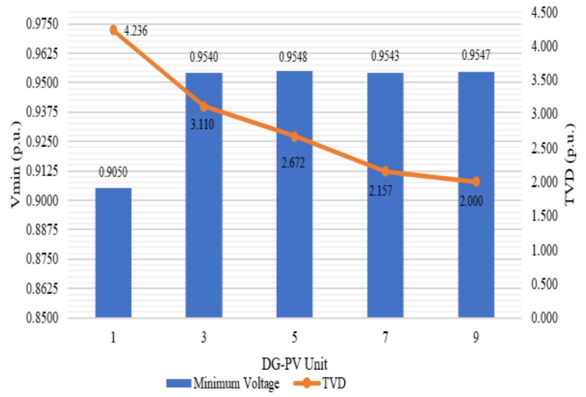

Fig. 7 Total Voltage Deviation and Minimum Bus Voltage Obtained for Multi-DGPV Installation using IIMFEP Technique in 118-Bus RDS.

This study demonstrates that the IIMFEP method beats EP, AIS, and MFO for multi-DGPV studies in terms of achieving the lowest real power losses. This study also illustrates that by adding several DGPVs to a system, the lowest voltage may be increased while the TVD is decreased; thus, it improves the voltage profile of the system. DG penetration level rate of 94.26 percent is required, resulting in a total installation of 9 DGPV with a total capacity of 21,406,22 kW. As the number of DGPVs increased, so did the penetration rate and total DGPV capacity installed.

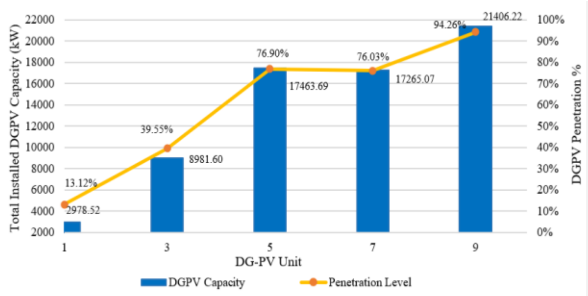

Fig. 6 The Total Installed DGPV capacity and Total DGPV Penetration Level Obtained for Multi-DGPV Installation using IIMFEP Technique in 118-Bus RDS.

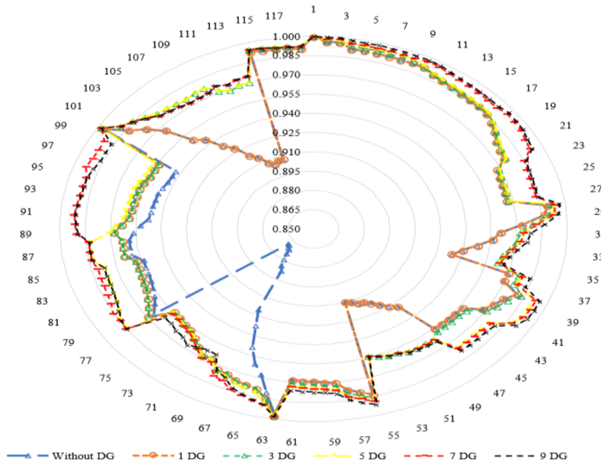

Fig. 8 Voltage Profile without DG Compensation and with 3 DGs Type I Installation using IIMFEP Technique in IEEE 118-Bus RDS.

F. Effect Of Load Variations On Multi-DGPV Installation

This part investigates the impact of multi-DGPV installation on the 118-Bus RDS during load changes, with the goal of minimizing total loss. The EP, AIS, MFO, and IIMFEP optimization techniques are utilized to determine the optimal placements and sizes of the three DGPV units on the IEEE 118-Bus RDS under load variations. Table 9 illustrates the system's total losses and minimum voltage for six distinct loading levels: 60%, 80%, 100%, 120%, 140%, and 160% from the base load value for uncompensated DG devices and with installations of three DGPVs in the system. Meanwhile, the optimal sizing and location with DGPVs installation under different load variations of the 118-Bus system are shown in Table 10.

The actual power losses on uncompensated DG devices in the 118-bus system are 434.97 kW when the load is lowered by 40% but climb to 3799.6 kW when the load is increased by about 60% of its base value. Meanwhile, when the load is lowered by 40% below the base load, the system's minimum voltage is 0.9253 p.u., which lowers more as the load increases. The minimum voltage is 0.7673 p.u. when the system is heavily loaded (60% above the base value).

When K=0.6, the IIMFEP technique provided the lowest overall power losses of 248.08 kW, compared to the MFO, AIS, and EP methods, which produced 186.99 kW, 311.57 kW, and 311.59 kW, respectively. According to Table 7, the ideal locations and sizes for DG1, DG2, and DG3 via IIMFEP are bus 37, bus 71, and bus 110, with 2073.8 kW, 1793.54 kW, and 1685.32 kW, respectively. When the load increased to approximately 60% of its base value, IIMFEP reported the lowest total system loss of 1926.25 kW, whereas EP, AIS, and MFO produced 2836.15 kW, 2741.03 kW, and 1952.34 kW, respectively. For a load factor of 1.6, the ideal locations and sizes for DG1, DG2, and DG3 via IIMFEP are bus 110, bus 37, and bus 71, with capacities of 4688.47 kW, 5696.4 kW, and 4989.73 kW, respectively. The results for other load factors can be referred at the same tables.

Increases in load factor will result in an increase in overall power losses for the 118-bus system, as depicted in Figure 9. For all load variations on a 118-bus system, the IIMFEP technique successfully achieves the lowest total power losses. When three DGPVs are integrated into the 118-bus system, total power loss is reduced from 434.97 kW to 248.08 kW, 800.42 kW to 448.3 kW, 1298.07 kW to 712.38 kW, 1946.08 kW to 1043.7 kW, 2768.87 kW to 1446.13 kW, and 3799.6 kW to 1926.25 kW, correspondingly, for load factor K=0.6, 0.8, 1.0, 1.2, 1.4, and 1.6 respectively using IIMFEP technique.

As illustrated in Figure 10, the recommended total DG size increases as the system's load increases. For all load variations in the system, the EP and AIS techniques generated larger total DG sizes than the MFO and IIMFEP techniques. However, the enormous size of DGs in the system does not guarantee minimum power loss. Regarding IIMFEP and MFO, they illustrate that more DG real power must be supplied when the load grows to counter the increase in total system losses. The optimal DG sizes created by each technique do not surpass the total real power consumption of the 118-bus system for all load variations.

Table 9. Comparison of Simulation Result of EP, AIS, MFO and IIMFEP for Multi-DGPV Installation for 118-Bus RDS under Load Variations with 20% Load Increment for Each Interval

Technique		Load Factor					
		K=0.6	K=0.8	K=1.0	K=1.2	K=1.4	K=1.6
Without DG	Total APL (kW)	434.97	800.42	1298.07	1946.08	2768.87	3799.60
	Total RPL (kVAr)	329.38	604.88	978.72	1463.54	2076.14	2839.09
	V_{min} p.u.	0.9253	0.8979	0.8688	0.8377	0.8041	0.7673
EP	Total APL (kW)	311.59	565.76	943.90	1395.28	1952.97	2836.15
	Total RPL (kVAr)	248.38	451.40	712.71	1055.20	1479.32	2372.58
	V_{min} p.u.	0.9474	0.9288	0.9115	0.8910	0.8694	0.8468

AIS	Total APL (kW)	311.57	565.70	944.36	1396.55	1926.25	2741.03
	Total RPL (kVAr)	248.38	451.41	713.47	1057.02	1471.64	2074.13
	V_{min} p.u.	0.9474	0.9288	0.9113	0.8907	0.8690	0.8531
MFO	Total APL (kW)	258.35	453.04	675.03	1048.68	1449.93	1952.34
	Total RPL (kVAr)	186.99	326.66	512.82	751.36	1035.16	1403.66
	V_{min} p.u.	0.9642	0.9525	0.9399	0.9377	0.9194	0.8996
IIMFEP	Total APL (kW)	**248.08**	**448.30**	**667.28**	**1043.70**	**1446.13**	**1926.25**
	Total RPL (kVAr)	177.63	320.13	507.05	745.59	1033.28	1380.19
	V_{min} p.u.	0.9642	0.9518	0.9392	0.9262	0.9131	0.8996

Table 10. The Optimal Sizing and Location with DGPV Installation under Different Load Variations of 118-Bus RDS

Technique		**Load Factor**					
		K=0.6	**K=0.8**	**K=1.0**	**K=1.2**	**K=1.4**	**K=1.6**
EP	Sizes of DGs (kW)/ Bus	2225.04 (68)	2966.72 (68)	2626.76 (106)	3152.73 (106)	3678.19 (106)	16211.71 (101)
		6748.20 (63)	8997.63 (63)	3125.78 (56)	3752.07 (56)	4377.41 (56)	7380.63 (67)
		1597.88 (112)	2130.50 (112)	4509.52 (67)	5412.50 (67)	6314.58 (67)	5023.63 (110)
AIS	Sizes of DGs (kW)/ Bus	2223.85 (68)	2962.09(68)	2592.02 (106)	3090.18 (106)	3580.63 (106)	8112.31 (73)
		6745.51 (63)	8985.50(63)	3106.23 (56)	3715.71 (56)	4334.39 (55)	4585.84 (109)
		1595.30 (112)	2121.81(112)	4486.23 (67)	5369.60(67)	6274.52(67)	6273.10 (42)
MFO	Sizes of DGs (kW)/ Bus	2073.76 (37)	1816.78 (40)	2702.30 (111)	3756.66 (109)	4400.02 (38)	5696.55 (37)
		1424.40 (118)	2410.06 (71)	3015.72 (49)	3675.47 (71)	4326.08 (71)	3633.56 (110)
		1793.48 (71)	2459.84 (109)	2985.47 (71)	3299.04 (40)	4423.87 (109)	4989.80 (71)
IIMFEP	Sizes of DGs (kW)/ Bus	2073.80 (37)	2779.34(37)	2978.57 (71)	3756.66 (109)	4424.02 (109)	4677.47 (110)
		1793.54 (71)	2410.13(71)	3119.86 (109)	3675.38 (71)	4326.25 (71)	5696.40 (37)
		1685.32 (110)	2459.79(109)	2883.17 (50)	4217.76 (37)	4951.64 (37)	4989.73 (71)

When the system is under light load (40 percent of normal load), the minimum voltage without DG compensation is 0.9253 p.u. When three DGPVs are optimally located in the system, the minimum voltage in the system is improved to 0.9474 p.u. using EP and AIS, and 0.9642 p.u. using MFO and IIMFEP, respectively. Meanwhile, under heavy load (60 percent of normal load), the system's minimum voltage increased from 0.7673 p.u. to 0.8468 p.u. via EP, 0.8531 p.u. via AIS, and 0.8996 p.u. via MFO and IIMFEP. Figure 11 shows the voltage profile of the uncompensated system under load variations. It can be seen that the voltage profile of the system is getting poorer as the real and reactive power load demand in the systems increases. The worst voltage profile occurs when the load factor is 1.6 of the base load, as depicted on the innermost side of Figure 11's radar graph.

Meanwhile, Figure 12 illustrates the voltage profiles of the compensated system with three DGPVs under load variations using the IIMFEP technique. The voltage profile of the compensated system is enhanced with the installation

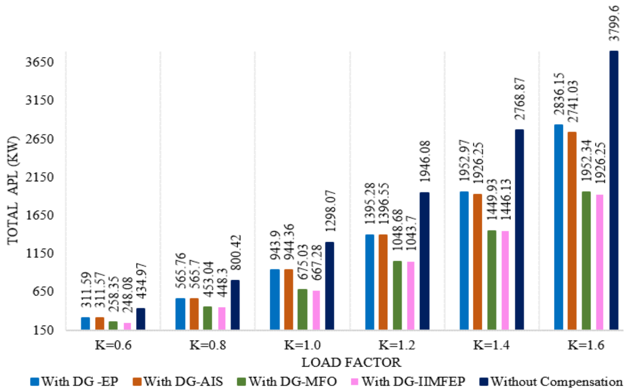

Fig. 9 Total APL with and without DGPV under Load Variations for IEEE 118-Bus RDS.

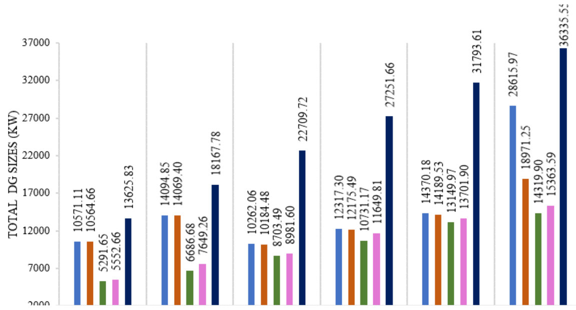

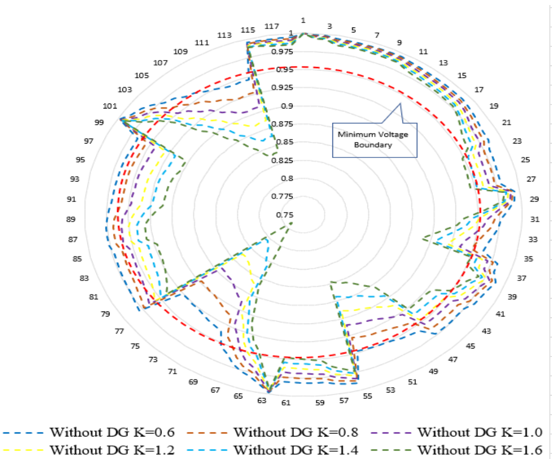

Fig. 11 Voltage Profile without DG Compensation for IEEE 118-Bus RDS under Load Variations

of three DGPVs in the system compared to without DG installation. As the load in the system increases from light to heavy load, even with three DGs installed, the system's minimum voltage deteriorates to the point where it is below the voltage limit for load factors of 1.0, 1.2, 1.4 and 1.6, respectively. Using the IIMFEP technique, the system's minimum voltage is 0.9642 p.u., 0.9518 p.u., 0.9392 p.u., 0.9262 p.u., 0.9131 p.u., and 0.8996 p.u. for load factors K=0.6, 0.8, 1.0, 1.2, 1.4, and 1.6, respectively.

This study reveals that the IIMFEP method achieves the lowest total APL among EP, AIS, and MFO methodologies for multi-DGPV investigations under load variations. As the system load is adjusted, the IIMFEP technique successfully identifies three DGPVs' ideal sizes and positions in a 118-Bus RDS. When the system load increased by 20%, from 60% of the base load to 160% of the base load, the overall power loss increased, the voltage profile of the system deteriorated, and the minimum bus voltage reduced. This

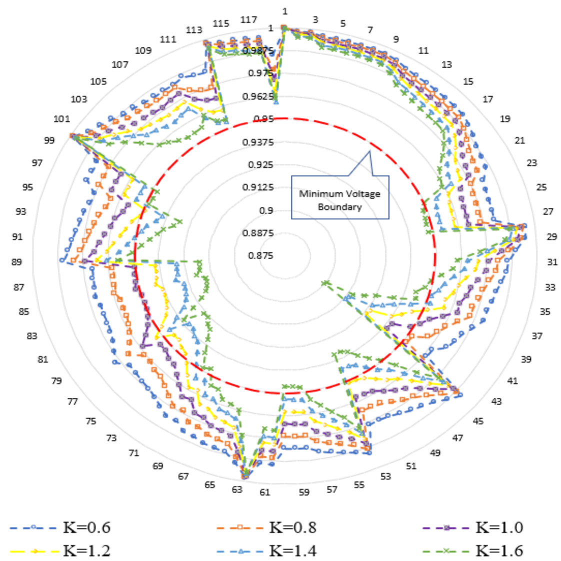

Fig. 12 Voltage Profile with DGPVs Compensation using IIMFEP for IEEE 118-Bus RDS under Load Variations

study demonstrates that for load factors of 0.6, 0.8, and 1.0, the installation of three DGPVs with optimal sizes and placements can reduce the system's power loss, raise the minimum bus voltage above the minimum voltage limitation, and improve the voltage profile of the system. As the system load exceeds the base load (1.2, 1.4, and 1.6), the installation of three DGPVs reduces the total APL and improves the voltage profile; however, the lowest voltage is still below the minimum voltage restriction. It is recommended to install more than three DGs in a 118-Bus RDS to fulfil the load demand in excess of the base load, hence lowering the total APL and maintaining the minimum bus voltage within the voltage limit.

G. Comparative Analysis of 118-Bus RDS

To further verify the efficacy of the proposed IIMFEP method in the 118-Bus system, simulation results are compared to those obtained using alternative methods, such as the Salp Swarm Algorithm (SSA), the Sine Cosine Algorithm (SCA), the Whale Optimization Algorithm (WOA), and the Grey Wolf Optimizer (GWO). Table 8 displays the results for the 118-Bus RDS system, including optimal DG placements and sizes derived from various approaches and proposed IIMFEP technique for base case condition. Based on Table 11, it can be observed that the IIMFEP technique achieves the lowest total APL when installing three, five, seven and nine DGPVs in 118-Bus RDS for base case conditions compared with SSA, SCA, WOA and GWO techniques.

Table 11. Comparison Results of IIMFEP, SSA, SCA, WOA and GWO for Multi-DGPV Installation in 118-Bus System

DG Units		IIMFEP	SSA	SCA	WOA	GWO
Three DGPVs	**DG sizes (kW)/Bus**	2978.57 (71), 3119.86 (109), 2883.17 (50)	3119.48 (109), 3540.47 (35), 2978.46 (71)	2271 (51), 2271 (75), 2857 (110)	2635.15 (50), 2929.31 (110), 3054.58 (71)	3276.87 (50), 2793.54 (71), 4111.73 (108)
	Total APL (kW)	**667.28**	677.57	694.82	668.62	688.16
Five DGPVs	**DG sizes (kW)/Bus**	2857.79 (71), 6454.16 (29), 2512.90 (50), 2520.11 (79), 3118.73 (109)	3235.43 (109), 2697.43 (72), 2596.26 (40), 2743.21 (50), 2491.06 (86)	2270.97 (28), 2590.65 (52), 3096.11 (108), 2710.78 (9), 2270.97 (73)	2497.05 (96), 2270.97 (41), 2431.06 (72), 2546.75 (51), 2544.52 (110)	3244.57 (70), 2624.47 (50), 2723.94 (36), 2505.74 (6), 4152.67 (108)
	Total APL (kW)	**581.57**	590.07	665.22	597.78	660.07
Seven DGPVs	**DG sizes (kW)/Bus**	2270.97 (40), 2699.48 (50), 2270.97 (96), 2869.17 (110), 2270.97 (80), 2270.97 (20), 2612.53 (71)	2352.27 (50), 3028.47 (30), 2270.97 (41), 2270.97 (91), 2575.73 (110), 2270.97 (102), 2443.66 (73)	2984.14 (81), 3780.11 (109), 2395.65 (73), 4205.28 (34), 5608.97 (6), 2767.46 (2), 3657.45 (3)	2316.27 (91), 2317.30 (50), 2317.19 (41), 2317.19 (73), 2317.19 (110), 2319.06 (21), 2317.44 (80)	3127.30 (50) ,2703.48 (72),2615 (6), 3743.63 (109), 2848.97 (79), 2405.49 (30), 2307.10 (19)
	Total APL (kW)	**527.07**	557.31	658.13	538.35	581.83
Nine DGPVs	**DG sizes (kW)/Bus**	2496.91 (30), 2270.97 (20), 2334.28 (50), 2270.97 (2), 2270.97 (91), 2351.28 (73), 2270.97 (40), 2868.88 (110), 2270.98 (79)	2396.62 (11),2335.62 (73), 2270.97 (89), 2282.79 (36), 2275.24 (50), 2270.97 (55), 3183.47 (109), 2270.97 (39), 2287.68 (79)	2270.97 (2), 3654.56 (34), 3647.84 (108), 2270.97 (5), 3098.27 (72), 2718.63 (29), 2270.97 (87), 2270.97 (2), 2270.97 (68)	2270.97 (30), 2270.97 (110), 2270.97 (40), 2270.97 (96), 2270.97 (5), 2270.97(74), 2270.97 (50), 2270.97 (103), 2270.97 (64)	3630.37 (2), 3801.39 (109), 2275.88 (14), 3158.58 (71), 2727.94 (79), 2614.27 (35), 2922.78 (4), 3413.24 (3), 2321 (4)
	Total APL (kW)	**511.43**	530.53	680.31	546.01	637.29

5. Conclusions

This study solves the optimal DGPV allocation problem in 118-Bus distribution networks using a newly upgraded method called IIMFEP. The issue under examination explores the optimal position, size, and number of DGs for integration into an RDS to accomplish a technical goal of total active power loss reduction while considering network and DG operational constraints. Then, the IIMFEP method is further evaluated to identify the size and locations of three DGs in the system based on load variations.

The suggested IIMFEP method was compared to EP, AIS, and MFO methods. The IIMFEP strategy beat the other three strategies in all cases, producing the lowest total APL and the highest PLRP rating. Using the IIMFEP method, the system's total APL is reduced to 1016.69 kW, 667.28 kW, 581.57 kW, 527.07 kW, and 511.43 kW when 1, 3, 5, 7, and 9 Type 1 DGs are installed, respectively. When the real and reactive power load demand varies between 60%, 80%, 100%, 120%, 140%, and 160% of the base load, the total APL of the system increases. The IIMFEP technique produces the lowest total APL, which is 434.97 kW, 800.42 kW, 667.28 kW, 1043.70 kW, 1446.13 kW, and 1926.25

kW, when three DGs are installed in the system with load factors of 0.6, 0.8, 1.0, 1.2, 1.4, and 1.6, respectively. As a result, it is feasible to conclude that the IIMFEP technique is an excellent solution for addressing large-scale technical challenges associated with optimal DG allocation in distribution networks.

ACKNOWLEDGMENT

The authors would like to acknowledge the Research Management (RMC) UiTM Shah Alam, Selangor, Malaysia and the Ministry of Higher Education, Malaysia (MOHE) for the financial support of this research. This research is supported by MOHE under Fundamental Research Grant Scheme (FRGS) with project code: FRGS/1/2019/TK04/UITM/01/1 and 600-IRMI/FRGS 5/3 (381/2019)

References

[1] S. K. Dash, S. Mishra, A. Y. Abdelaziz, M. L. Alghaythi, and A. Allehyani, "Optimal Allocation of Distributed Generators in Active Distribution Networks Using a New Oppositional Hybrid Sine Cosine Muted Differential Evolution Algorithm," *Energies (Basel)*, vol. 15, no. 6, Mar. 2022, doi: 10.3390/en15062267.

[2] M. Ntombela, K. Musasa, and M. C. Leoaneka, "Power Loss Minimization and Voltage Profile Improvement by System Reconfiguration, DG Sizing, and Placement," *Computation*, vol. 10, no. 10, p. 180, Oct. 2022, doi: 10.3390/computation10100180.

[3] L. C. Kien, T. T. Bich Nga, T. M. Phan, and T. T. Nguyen, "Coot Optimization Algorithm for Optimal Placement of Photovoltaic Generators in Distribution Systems Considering Variation of Load and Solar Radiation," *Math Probl Eng*, vol. 2022, 2022, doi: 10.1155/2022/2206570.

[4] G. Tahiliani and A. R. Gupta, "Voltage Profile improvement by optimal DG allocation using atom search optimisation in radial and mesh distribution system," *International Journal of Engineering, Science and Technology*, vol. 14, no. 3, pp. 112–121, Aug. 2022, doi: 10.4314/ijest.v14i3.13s.

[5] J. M. Home-Ortiz, M. Pourakbari-Kasmaei, M. Lehtonen, and J. R. Sanches Mantovani, "Optimal location-allocation of storage devices and renewable-based DG in distribution systems," *Electric Power Systems Research*, vol. 172, pp. 11–21, Jul. 2019, doi: 10.1016/j.epsr.2019.02.013.

[6] P. Prakash, D. C. Meena, H. Malik, M. A. Alotaibi, and I. A. Khan, "A Novel Analytical Approach for Optimal Integration of Renewable Energy Sources in Distribution Systems," *Energies (Basel)*, vol. 15, no. 4, Feb. 2022, doi: 10.3390/en15041341.

[7] N. R. Godha Dagade, V. N. Bapat, and I. Korachagaon, "Improved ACO for Planning and Performance Analysis of Multiple Distributed Generations in Distribution System for Various Load Models," in *2020 2nd International Sustainability and Resilience Conference: Technology and Innovation in Building Designs*, Nov. 2020. doi: 10.1109/IEEECONF51154.2020.9319962.

[8] M. J. Afzal, A. Arshad, S. Ahmed, S. bin Tariq, and S. A. A. Kazmi, "A review of DGs and FACTS in power distribution network: Methodologies and objectives," in *2018 International Conference on Computing, Mathematics and Engineering Technologies: Invent, Innovate and Integrate for Socioeconomic Development, iCoMET 2018 - Proceedings*, Apr. 2018, vol. 2018-January, pp. 1–7. doi: 10.1109/ICOMET.2018.8346405.

[9] M. Pesaran H.A, P. D. Huy, and V. K. Ramachandaramurthy, "A review of the optimal allocation of distributed generation: Objectives, constraints, methods, and algorithms," *Renewable and Sustainable Energy Reviews*, vol. 75. Elsevier Ltd, pp. 293–312, 2017. doi: 10.1016/j.rser.2016.10.071.

[10] W. L. Theo, J. S. Lim, W. S. Ho, H. Hashim, and C. T. Lee, "Review of distributed generation (DG) system planning and optimisation techniques: Comparison of numerical and mathematical modelling methods," *Renewable and Sustainable Energy Reviews*, vol. 67. Elsevier Ltd, pp. 531–573, Jan. 01, 2017. doi: 10.1016/j.rser.2016.09.063.

[11] R. O. Bawazir and N. S. Cetin, "Comprehensive overview of optimizing PV-DG allocation in power system and solar energy resource potential assessments," *Energy Reports*, vol. 6. Elsevier Ltd, pp. 173–208, Nov. 01, 2020. doi: 10.1016/j.egyr.2019.12.010.

[12] P. V. K. Babu and K. Swarnasri, "Optimal integration of different types of DGs in radial distribution system by using Harris hawk optimization algorithm," *Cogent Eng*, vol. 7, no. 1, Jan. 2020, doi: 10.1080/23311916.2020.1823156.

[13] Z. B. A. Hamid, S. Jipinus, I. Musirin, M. M. Othman, and R. H. Salimin, "Optimal sizing of distributed generation using firefly algorithm and loss sensitivity for voltage stability improvement," *Indonesian Journal of Electrical Engineering and Computer Science*, vol. 17, no. 2, pp. 720–727, 2019, doi: 10.11591/ijeecs.v17.i2.pp720-727.

[14] A. Eid, S. Kamel, and L. Abualigah, "Marine predators algorithm for optimal allocation of active and reactive power resources in distribution networks," *Neural*

Comput Appl, 2021, doi: 10.1007/s00521-021-06078-4.

[15] S. A. Shaaya, I. Musirin, S. I. Sulaiman, M. H. Mansor, and S. A. S. Mustaffa, "Effect of DG types and penetration level in transmission system using hybrid optimization technique for loss control," *International Journal of Emerging Trends in Engineering Research*, vol. 8, no. 1 Special Issue 1, pp. 1–6, 2020, doi: 10.30534/ijeter/2020/0181.12020.

[16] R. Sanjay Kumar and N. Anbuselvan, "Power Factor Improvement of Wind based DGs in the Distribution System Using (Fruit Fly and Cat Swarm) Optimization Techniques by Reducing the Harmonics," 2021.

[17] E. A. Al-Ammar *et al.*, "ABC algorithm based optimal sizing and placement of DGs in distribution networks considering multiple objectives," *Ain Shams Engineering Journal*, vol. 12, no. 1, pp. 697–708, Mar. 2021, doi: 10.1016/j.asej.2020.05.002.

[18] S. A. S. Mustaffa, I. Musirin, M. M. Othman, M. K. M. Zamani, and A. Kalam, "Chaotic local search based algorithm for optimal DGPV allocation," *Indonesian Journal of Electrical Engineering and Computer Science*, vol. 11, no. 1, pp. 113–120, Jul. 2018, doi: 10.11591/ijeecs.v11.i1.pp113-120.

[19] T. L. Duong, P. T. Nguyen, N. D. Vo, and M. P. Le, "A newly effective method to maximize power loss reduction in distribution networks with highly penetrated distributed generations," *Ain Shams Engineering Journal*, vol. 12, no. 2, pp. 1787–1808, Jun. 2021, doi: 10.1016/j.asej.2020.11.003.

[20] S. Kawambwa, R. Mwifunyi, D. Mnyanghwalo, N. Hamisi, E. Kalinga, and N. Mvungi, "An improved backward/forward sweep power flow method based on network tree depth for radial distribution systems," *Journal of Electrical Systems and Information Technology*, vol. 8, no. 1, Dec. 2021, doi: 10.1186/s43067-021-00031-0.

[21] D. Issicaba and J. Coelho, "Evaluation of the forward-backward sweep load flow method using the contraction mapping principle," *International Journal of Electrical and Computer Engineering*, vol. 6, no. 6, pp. 3229–3237, 2016, doi: 10.11591/ijece.v6i6.11303.

[22] C. S. M. anoj Gupta, "Review of Forward & Backward Sweep Method for Load Flow Analysis of Radial Distribution System," *International Journal of Advanced Research in Electrical, Electronics and Instrumentation Engineering*, vol. 04, no. 06, pp. 5595–5599, Jun. 2015, doi: 10.15662/ijareeie.2015.0406049.

[23] B. M'hamdi, M. Teguar, and B. Tahar, "Optimal DG unit placement and sizing in radial distribution network for power loss minimization and voltage stability enhancement," *Periodica polytechnica Electrical engineering and computer science*, vol. 64, no. 2, pp. 157–169, Apr. 2020, doi: 10.3311/PPEE.15057.

[24] S. Kumar, K. Krishna Mandal, M. Ghosh, S. Kumar, S. Mandal, and K. Mandal, "Optimal Sizing and Placement of DG Units in Radial Distribution System Using Cuckoo Search Algorithm." [Online]. Available: http://www.ripublication.com

[25] T. Yuvaraj and K. Ravi, "Multi-objective simultaneous DG and DSTATCOM allocation in radial distribution networks using cuckoo searching algorithm," *Alexandria Engineering Journal*, vol. 57, no. 4, pp. 2729–2742, Dec. 2018, doi: 10.1016/j.aej.2018.01.001.

[26] T. Yuvaraj, K. Ravi, and K. R. Devabalaji, "Optimal Allocation of DG and DSTATCOM in Radial Distribution System Using Cuckoo Search Optimization Algorithm," *Modelling and Simulation in Engineering*, vol. 2017, 2017, doi: 10.1155/2017/2857926.

[27] D. Zhang, Z. Fu, and L. Zhang, "An improved TS algorithm for loss-minimum reconfiguration in large-scale distribution systems," *Electric Power Systems Research*, vol. 77, no. 5–6, pp. 685–694, Apr. 2007, doi: 10.1016/j.epsr.2006.06.005.

[28] H. R. E H Bouchekara, "Comprehensive Review of Radial Distribution Test Systems Optimal Coordination of Directional Overcurrent Relays View project Design of Hybrid Nanogrid in the Desert Camps of Hafr Al-Batin City View project", doi: 10.36227/techrxiv.12578648.v1.